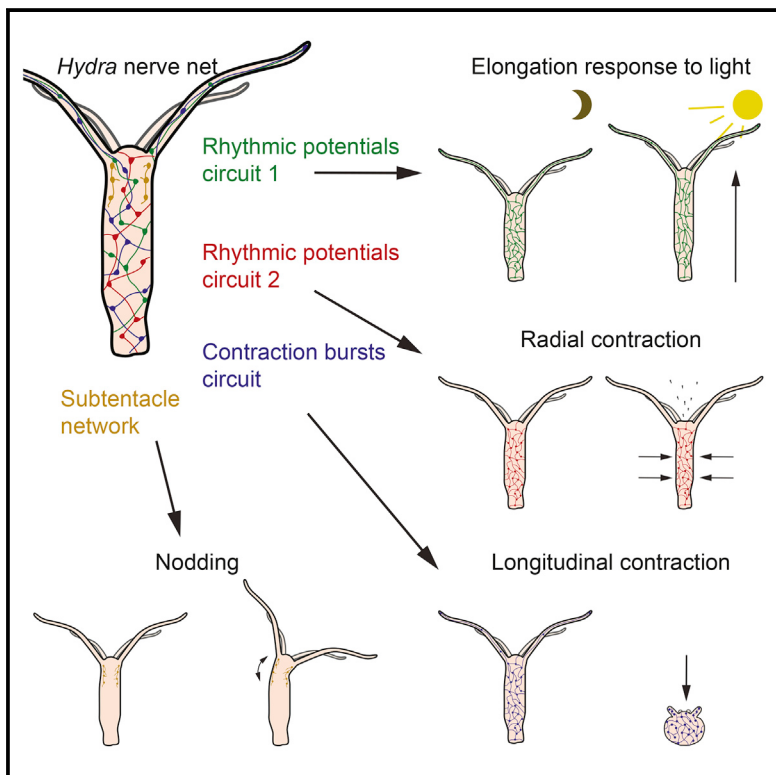


Graphical Abstract



Authors

Christophe Dupre, Rafael Yuste

Correspondence

cd2597@columbia.edu

In Brief

The nervous system of *Hydra* is traditionally described as made of two nerve nets. By using calcium imaging, Dupre and Yuste demonstrate the existence of multiple circuits within these nerve nets and show with which behavior they are associated.

Highlights

- Introduction of *Hydra* as a model system for neural circuits
- Functional circuits of four behavioral responses
- First complete Brain Activity Map achieved

Non-overlapping Neural Networks in *Hydra vulgaris*

Christophe Dupré^{1,2,*} and Rafael Yuste¹

¹Neurotechnology Center, Department of Biological Sciences and Neuroscience, Columbia University, New York, NY 10027, USA

²Lead Contact

*Correspondence: cd2597@columbia.edu

<http://dx.doi.org/10.1016/j.cub.2017.02.049>

SUMMARY

To understand the emergent properties of neural circuits, it would be ideal to record the activity of every neuron in a behaving animal and decode how it relates to behavior. We have achieved this with the cnidarian *Hydra vulgaris*, using calcium imaging of genetically engineered animals to measure the activity of essentially all of its neurons. Although the nervous system of *Hydra* is traditionally described as a simple nerve net, we surprisingly find instead a series of functional networks that are anatomically non-overlapping and are associated with specific behaviors. Three major functional networks extend through the entire animal and are activated selectively during longitudinal contractions, elongations in response to light, and radial contractions, whereas an additional network is located near the hypostome and is active during nodding. These results demonstrate the functional sophistication of apparently simple nerve nets, and the potential of *Hydra* and other basal metazoans as a model system for neural circuit studies.

INTRODUCTION

Understanding the function of any nervous system is a daunting task, given the number of neurons involved and the difficulty in measuring and analyzing their activity. Cnidarians, as a sister group of bilaterians, are extant representatives of some of the earliest animals in evolution to have nervous systems, and thus offer an apparent simplicity that could help illuminate the structural and functional design principles of neural circuits. Among cnidarians, *Hydra* is convenient to maintain and manipulate in a laboratory and, consequently, has been studied for more than 300 years [1]. The nervous system of *Hydra* is composed of a few hundred to a few thousand neurons, depending on the size of the animal [2]. Two main types of neurons have been reported: sensory cells, exposed to the external or gastric environment, and ganglion cells, which form a two-dimensional lattice known as a nerve net [3, 4]. *Hydra*'s nerve net actually has two separate components: one in the endoderm and one in the ectoderm. The morphology of both sensory cells and ganglion cells can vary, in terms of the size of their cell body and the ramification of their neurites [5].

The function of the nerve nets in *Hydra* is poorly understood. Extracellular recordings have reported multiple types of electrical activity, some of which are associated with motion or occur

in response to sensory stimulation. Specifically, longitudinal contraction of the ectoderm, which reduces the animal down to a tight ball, is associated with a type of extracellular electrical signals named longitudinal contraction bursts (CBs) [6]. Tentacles sometimes also generate electrical pulses (tentacle pulses), found during contractions [7, 8]. However, in addition, *Hydra* displays robust spontaneous electrical activity, i.e., activity in the apparent absence of any external stimulus and, sometimes, also in the absence of any clear behavior. One example of this is rhythmic electrical potentials [6, 9], which have been thought to propagate in the endoderm of the animal [10] and to increase in frequency during elongation of the body column [6]. Activation of the endoderm by rhythmic potentials (RPs) is thought to cause radial contraction (reduction of the radius of the animal) and therefore elongation [11, 12].

Hydra has a limited and well-characterized behavioral repertoire, including photic response and feeding. A dark-habituuated *Hydra* that is exposed to light will respond by elongating its body toward it, bending its hypostome-tentacle junction to produce a motion reminiscent of nodding [13, 14], and eventually moving toward the light source by somersaulting [15]. Feeding includes a combination of tentacle motion to spear and paralyze the prey with nematocysts in order to bring the prey toward the mouth, which opens to ingest it [16]. A few hours after ingestion, the content of the body column is expelled through the mouth by a quick radial (as opposed to longitudinal) contraction of the body column after the mouth has opened [17].

Elucidation of the links between neuronal activity, anatomy, and behavior in *Hydra* has been difficult because of technical limitations. Single-cell recording approaches are difficult because *Hydra* neurons are small and scattered [18], although intracellular recordings reveal action potentials [19]. Extracellular studies have provided detailed descriptions of electrical signals but could not link them to a particular cell type. In fact, whether RPs and longitudinal CBs are conducted by neurons or by the muscle/epithelial cells is still under debate [10, 20, 21], and surgical isolations indicate that they can propagate along both axes of the epithelium [8]. Also, extracellular recordings, which could be more akin to electromyograms, can be disrupted by the motion of the animal [9], and therefore cannot be carried out for certain types of behavior. Accordingly, one does not know how many neural circuits exist in the nervous system of *Hydra* and in what behavior each of them participates.

The application of modern molecular methods to *Hydra* has the potential to greatly advance our understanding of these essential neurobiological questions. In particular, the recent sequencing of *Hydra* has revealed a surprisingly rich genome [22]. Indeed, in spite of its basal metazoan lineage, the *Hydra* genome is endowed with more than 20,000 genes, including

an extensive complement of neuronal molecular families such as sodium, potassium, and calcium channels and receptors for glutamate, GABA, dopamine, 5-hydroxytryptamine, and many peptides. Many of these molecules are even present in animals that are evolutionarily more basal than cnidarians, such as the poriferans (sponges) [23]. Also, stable transgenic lines have been achieved [24], enabling the use of a large range of modern molecular tools. Among these tools, genetically encoded calcium indicators are particularly well suited for functional studies of the *Hydra* nerve net for many reasons. First, calcium imaging can track the action-potential activity of neuronal populations [25]. Second, the small size of *Hydra* (500 µm to 1.5 cm in length) makes it possible to have an entire animal under the field of view of a traditional microscope. Third, *Hydra* is transparent and its scattered nerve-net organization (disadvantageous for electrophysiological recordings) is advantageous for imaging. Indeed, it is rare that two neurons optically overlap during imaging, so it is therefore easier to obtain single-neuron resolution. Fourth, *Hydra* does not age [26], so the same animal can be used in an indefinite number of experiments. This can reduce the number of confounding factors and make statistical interpretation more accurate. Fifth, *Hydra* regenerates, which makes it more robust against photodamage. Other cnidarians are available, such as *Hydractinia*, *Aglantha*, and *Nematostella*. These animals offer various advantages, such as the broad range of genetic tools that are available in *Nematostella* [27]. In spite of the fact that these species might not have the same optical advantages as *Hydra*, running similar experiments in them would offer exciting comparative perspectives between the nervous system of anthozoans (e.g., *Nematostella*) and hydrozoans (e.g., *Hydra*). To take advantage of these properties and explore the possibility of performing neural circuit studies of *Hydra*, we created a line expressing a calcium indicator (GCaMP6s) in neurons. Using it, we attempted to link neuronal activity with the anatomy of the nerve net and the behavior of the animal.

RESULTS

Imaging the Complete Activity of the Nervous System of *Hydra*

In order to record the activity of the entire nervous system of *Hydra* simultaneously, we first generated a line of transgenic animals expressing a genetic calcium indicator and then developed a method to image whole individuals. To generate the transgenic line, we modified a plasmid initially designed by R. Steele (UC Irvine; Addgene catalog no. 34789) [28] that expresses GFP under the control of an actin promoter. In the sequence of this plasmid, we substituted GCaMP6s for GFP (see the *Supplemental Information*). We then injected the plasmid into fertilized *Hydra* eggs (Figure 1A) according to an established procedure [29] (see also *Supplemental Experimental Procedures*), with the goal of incorporating the plasmid into the interstitial cell lines, which give rise to the neuronal lineage.

Animals generated were mosaic, with transgenic stem cells randomly scattered throughout the body. By repeatedly selecting buds that formed on a region of the parent that has a higher concentration of transgenic stem cells than the rest of the body of the parent, we progressively increased the percentage of transgenic neurons in our colony. Once the percentage of trans-

genic neurons seemed to have reached a steady state, we measured it by immunostaining animals for GCaMP6s (using a GFP antibody) and acetylated alpha-tubulin, a pan-neuronal marker [30]. In these animals, 96% ± 3% (SEM) of cells positive for acetylated alpha-tubulin also expressed GCaMP6s (see Figure S1). Because it is likely that a small percentage of neurons might not have been stained for GFP and/or for anti-acetylated alpha-tubulin during the immunohistochemistry procedure, we concluded that the transgenic lines expressed GCaMP6s in essentially all of its neurons.

To image the activity of every neuron in the animal, we mounted specimens between two coverslips separated by a 100-µm spacer, which is the average width of a small *Hydra* (Figure 1B), and imaged in wide-field mode at a maximum 33-Hz frame rate (Movie S1; cf. *Experimental Procedures*). In such a preparation, the animal can be considered as a hollow cylinder that is imaged from the side, between the top coverslip (top layer in Figure 1B) and the bottom coverslip (bottom layer in Figure 1B). Consequently, we expected to see two layers of neurons (the two sides of the cylinder) slide on top of each other as the animal is moving in this chamber. Indeed, we could identify the two body walls by measuring the trajectory of eight neurons in a given region of interest and plotting these trajectories on top of each other (Figure 1C, left and middle panels). Accordingly, the eight trajectories essentially followed two different directions corresponding to the motion of the two layers of the animal. Moreover, we could detect calcium transients from neurons in both layers (Figure 1C, right panel). We ruled out the possibility that these fluorescence transients come from motion of the cells in and out of focus by comparing them to the signal we acquired from animals expressing GFP (rather than GCaMP6s) in neurons (Figure S2). For these reasons, we can conclude that our preparation allows us to image neuronal activity through the entire animal simultaneously.

In order to extract neuronal activity in spite of the motion of the animal, we manually tracked the trajectory of each neuron and measured its fluorescence intensity at each frame (cf. *Experimental Procedures*; Figure 1D; Movie S2). Additionally, we attempted to correlate calcium signal with electrical activity of the neurons by approaching extracellular electrodes (Figure 2A). We were not able to record the electrical activity of CB neurons, because whenever they fired, the electrical signal generated by the contracting muscles overwhelmed any other signal (Figure 2B). However, we were able to record electrical signals from RP neurons, because they can occur when the animal does not move. The calcium transients we observed all had the same amplitude, and the electrical activity that corresponded to them always involved a single spike (Figures 2C and 2D). Therefore, each RP calcium transient most likely corresponded to one action potential.

Using these traces for each neuron, we built raster plots representing the activity of every neuron over hundreds of frames (Figure 1D). Note that each animal can have a different number of neurons, as *Hydra* can grow and shrink depending on its food intake [2]. In addition, we tested how fast and for how long we could image these animals in our preparation. The duration of recording was limited by photobleaching and phototoxicity, which we assessed by measuring fluorescence intensity and neuronal activity, respectively. The speed of recording in

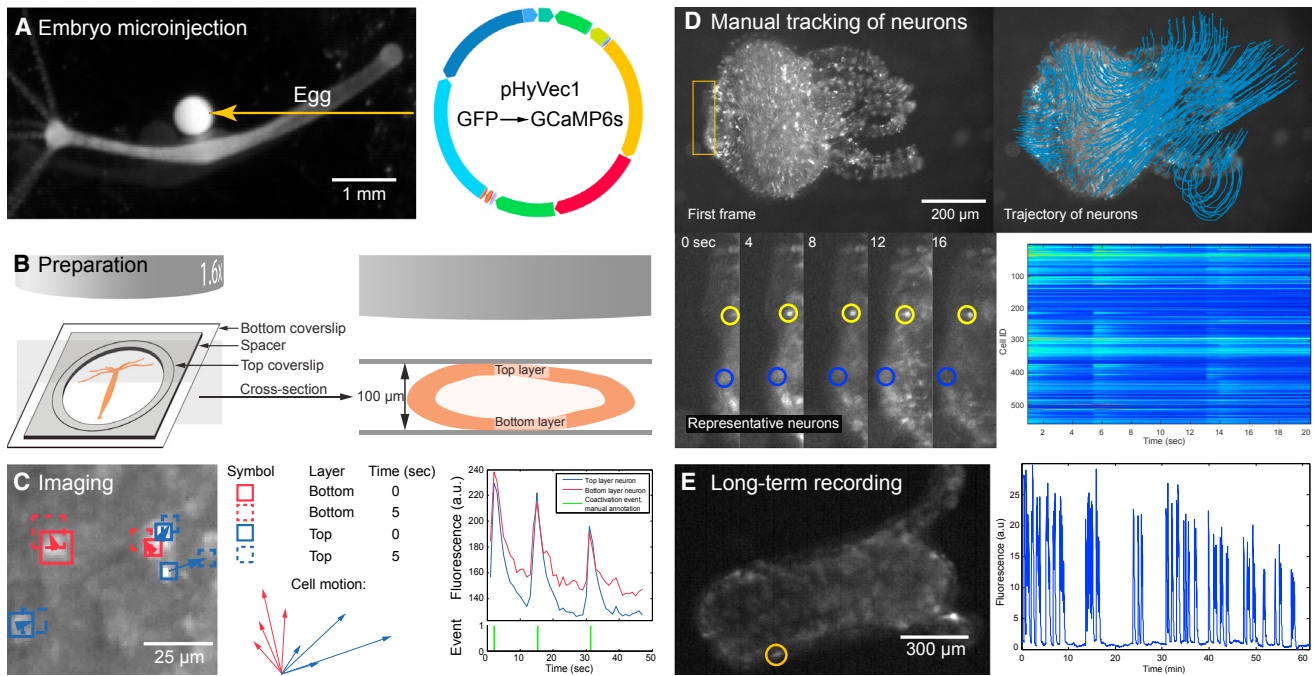


Figure 1. Imaging the Entire Nervous System Activity of *Hydra*

(A) To create the transgenic line, we injected into fertilized *Hydra* eggs (left) a plasmid that causes expression of GCaMP6s (right).
(B) Imaging preparation (left) and sample cross-section (right).
(C) Left: trajectory of five representative neurons. Middle: close-up of the trajectory of the eight tracked neurons, showing a difference in direction of the neurons of the top layer (blue) versus the neurons of the bottom layer (red). Right: single calcium spikes in neurons from both layers (top; see also Figure S2), with manual detection of coactivation events (bottom).
(D) First frame (top left), trajectory of all neurons (top right), close-up of the position of two representative neurons (bottom left), and fluorescence (bottom right) of all of the detected neurons during a typical recording. Measurements were made of the first 20 s (real time, i.e., 1.6 s of movie time) of Movie S1.
(E) Entire animal (left) imaged for more than 1 hr at 30 frames/s, with fluorescence signal (right) coming from the cell circled in yellow.
See also Figures S1, S2, and S4 and Movies S1 and S2.

our preparation was limited by the minimum acquisition time of the camera (30 ms). At this maximum speed, it was possible to continuously record neuronal activity for more than 1 hr without any apparent toxicity and little bleaching (Figure 1E). Because our staining indicates that every neuron was transgenic and our recording technique could image both layers of the animal, we believe to be close to imaging the activity of every neuron of *Hydra* simultaneously. Using these recordings, we classified the neurons of *Hydra* according to their morphologies, activity patterns, or any behavior observed.

Functional Networks of Neurons in *Hydra*

We define functional networks as groups of neurons that participate in a common function, such as a particular behavior. Among these functional networks, we observed three of them where neurons spanning the entire body of the animal were coactive (Figure 3A, red, green, and blue dots). Here, we define “coactive” as firing within the same 100-ms frame (Movie S1), acknowledging that with a higher temporal resolution we might be able to measure a delay between the activation of different neurons. Interestingly, these three networks were non-overlapping, i.e., any neuron belonging to one network did not belong to any of the other two networks. Additionally, we observed small functional networks of neurons located under the tentacle-hypo-

stome junction and individual neurons showing slower calcium transients rather than spikes (Figure 3A, yellow dots). We extracted every spike and slow calcium transient of the neurons recorded in a segment of the movie (Figure 3B). Accordingly, we reported in that segment a total of 14 activity epochs, 4 of them belonging to the coactive circuits.

One of the coactive networks involved neurons that became active during a longitudinal CB, which is one of the most commonly described behaviors of *Hydra* [9, 31]. Such bursts happened on average once every 4.4 min (± 53 s [SEM], $n = 6$ animals). In addition, we found networks of neurons active spontaneously, apparently corresponding to the RPs [9]. Unexpectedly, we found not one but two independent networks of cells generating these RPs (Figure 3A, green and red dots), which we named RP1 and RP2 and which fired on average once every 167 s (± 102 s [SEM], $n = 8$ animals) and 143 s (± 21 s [SEM], $n = 8$ animals), respectively.

Interactions between RPs and longitudinal CBs have been described previously [14]. Because they only assumed the existence of one RP system, we explored whether this was true for both RP networks. To examine this, we extracted the activation events of the CB, RP1, and RP2 in longer movies (up to 1 hr) in multiple animals and computed their cross-correlation (see the *Supplemental Experimental Procedures*). Indeed, RP1 showed

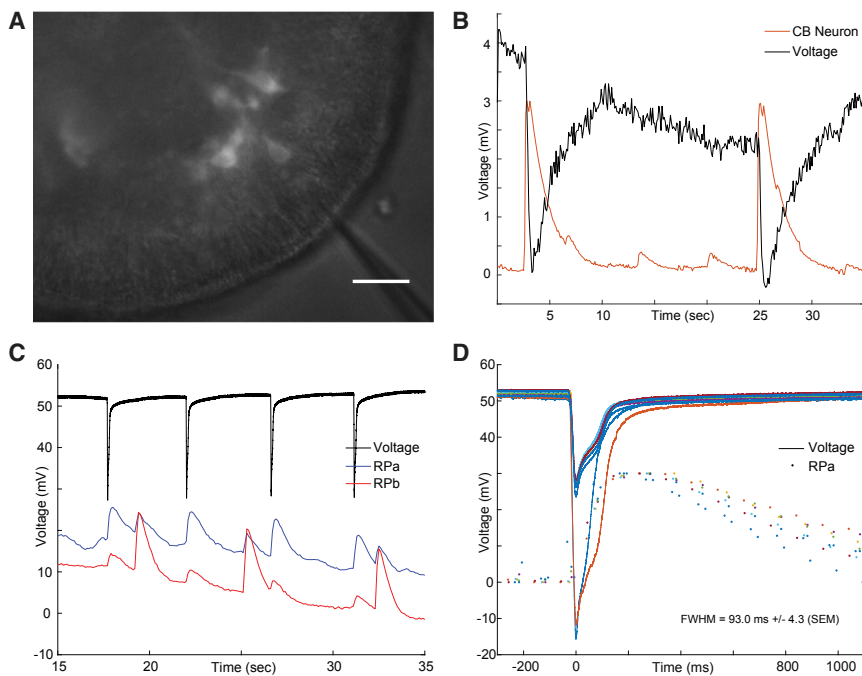


Figure 2. Simultaneous Recording of Electrical Activity and Calcium Imaging

(A) Preparation (scale bar, 20 μm). Electrode comes from the bottom and is slightly out of focus. (B) Extracellular electrode placed near a CB neuron, with fluorescence signal recorded from that neuron. Contractions produce overwhelming electrical signal. (C) Extracellular electrode placed close to a neuron from one RP network (RPa, which could be either RP1 or RP2) and far from a neuron from the other RP network (RPb). Accordingly, the spikes recorded in electrical activity match calcium spikes of neuron A (blue trace), but not neuron B (red trace). Note that there is cross-contamination between the fluorescence signals from neurons A and B, but one can distinguish them because of their amplitude difference (large spikes in neuron A result in small spikes in neuron B, and vice versa). (D) Superimposition of nine spikes from extracellular recording (top) and their corresponding calcium traces (bottom) for neuron A. The color of each electrical trace matches the color of the corresponding fluorescence trace. FWHM, full width at half maximum.

In (B)–(D), fluorescence traces are in a.u.

short-term interruptions when CBs became active (see arrows under the spike train in Figure 3C), which results in a dip at $t = 0$ in the cross-correlogram between RP1 and CB (Figure 3C, middle) and a decrease in RP1 frequency when CB frequency increases (cf. leftward inclination of the loops in Figure 3C, right). This indicates an antagonistic interaction between RP1 and CB and was present in seven animals (Figure 3D, middle). At the same time, no detectable relationship was found between RP1 and RP2 (Figure 3D, left) or between RP2 and CB (Figure 3D, right).

RP1 and CB Networks Are Ectodermal, Whereas RP2 Is Endodermal

We then examined the anatomical characteristics of the three widespread networks. Because neurons of a given network fire within the same frame (up to 30 ms in our fastest recordings), we assumed they must be connected into the same circuits via either chemical or electrical synapses. Because no neuronal connection has been described in *Hydra* between the endodermal and the ectodermal nerve net [32], we assumed that each RP1, RP2, and CB can only exist in one nerve net (either endodermal or ectodermal). We reasoned that the CB system should be in the ectoderm because ectodermal neurons innervate the longitudinal (vertical) muscle fibers of the ectodermal skin cells in order to cause longitudinal contractions. In addition, previous studies showed that the RPs exist in the endodermal nerve net [10] and cause contractions of the endoderm [12], which has been interpreted as producing elongation of the body column of the animal [11], because endodermal muscle cells are arranged circularly (horizontally). However, if RPs were generated by the endodermal nerve net, they would not be able to interact with CB neurons (as shown in Figure 3D), which are in the ectoderm. Thus, we hypothesized that RP1 is in the ectoderm, which allows it to interact with CB, whereas

RP2 should be in the endoderm, which prevents it from interacting with CB and RP1.

To test this hypothesis, we measured the presence of neurons belonging to the three networks in regions of our recordings that only contain the ectoderm of the animal, by taking advantage of the fact that, in our preparation, the animal is laid flat between two coverslips. Thus, when imaged from the objective, there is an area at the edge of the animal composed of ectoderm only, whereas the rest of the animal is a superimposition of both endoderm and ectoderm (dashed lines in Figure 4A). Accordingly, we found only RP1 neurons in areas containing ectoderm only (arrows in Figure 4A), whereas we found RP1 and RP2 neurons in areas containing both endoderm and ectoderm. We concluded that RP1 is in the ectodermal nerve net, whereas RP2 is in the endodermal nerve net.

We then tested whether neurons of RP1, RP2, and CB had different morphological features by comparing their soma size, number of primary neurites, and orientation of primary neurites (Figure 4B). We also measured these parameters for the individual neurons that did not participate in these three networks (“other” cells). The somata of CB neurons were larger when compared to all other categories ($10.73 \pm 0.62 \mu\text{m}$ [SEM]; $p < 0.01$, unpaired t test) (Figure 4C). Meanwhile, the number of primary neurites was higher ($p < 0.01$, unpaired t test) in RP2 neurons (3.2 ± 0.1) than in RP1 (2.78 ± 0.1), CB (2.9 ± 0.06), and other neurons (0.86 ± 0.2) (Figure 4D). The number of primary neurites of the other neurons was significantly smaller than for all other networks ($p < 0.01$, unpaired t test). Some of these neurons possessed one short branch (Figure 4B), a feature that is very characteristic of the sensory neurons, which have been reconstructed from serial-section electron microscopy [3]. The orientation of the primary neurites was also measured (Figure 4E), by using the oral-aboral axis as a reference (top-left panel). No specific orientation was found for any of the three major networks.

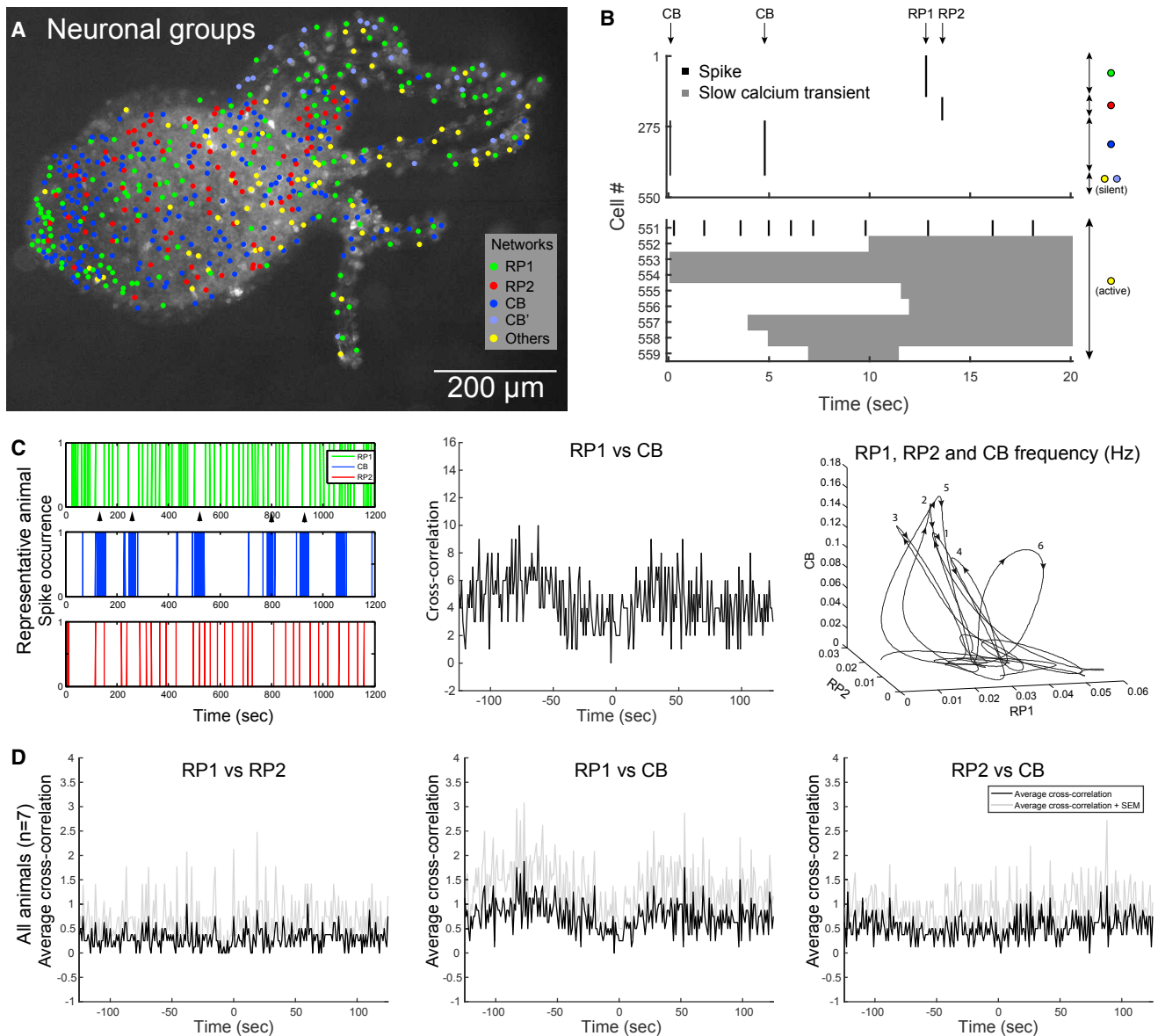


Figure 3. The Nervous System of *Hydra* Includes Three Major Non-Overlapping Networks

(A) Topographical distribution of neurons in *Hydra* (same dataset as Figure 1D), grouped into five categories: rhythmic potential 1 (RP1; green), rhythmic potential 2 (RP2; red), longitudinal CBs (dark and light blue), and other neurons (others; yellow). CB' indicates neurons of the tentacles that did not fire during the two CB events of this time window but fired during another CB event.

(B) Spikes (black) and slow calcium transients (gray) of the 559 cells shown in (A). Neurons are grouped by identity (colored dots on the right), and activity events are marked with arrows (top). Note the difference in scale between the y axis of the top and bottom plots, due to the large number of neurons belonging to RP1, RP2, and CB. Also, note that the two activity epochs labeled as CB are the last two spikes of a longitudinal CB.

(C) Left: spiking activity of the three networks in one representative animal. Each spike represents the coactivation of the neurons of one network (RP1, RP2, or CB). Arrows indicate a decrease in RP1 frequency during a longitudinal CB. Middle: cross-correlation between RP1 and CB. Right: plot of the firing frequency over time of the three networks. Numbers indicate longitudinal CBs.

(D) Cumulated (over seven animals) cross-correlation between RP1 and RP2 (left), RP1 and CB (middle), and RP2 and CB (right).

To further identify the spatial structure of the three networks, we first examined the overall distribution of neurons, finding that the overall density of neurons was higher in the hypostome ($3,679 \pm 401$ neurons/mm²) than in any other part of the animal ($p < 0.05$, paired t test, $n = 5$) and higher in the peduncle ($2,668.5 \pm 264$) than in the body column ($1,339.7 \pm 234$) ($p < 0.05$, paired t test,

$n = 5$; Figure 4F). These measurements match previous studies [5, 33], where the authors dissociated specific parts of *Hydra* (hypostome, body column, and peduncle) and measured the ratio between neurons and skin cells in each part. Other studies using staining methods came to similar conclusions [34–37]. Using these measurements, we calculated that CB and RP1 neurons

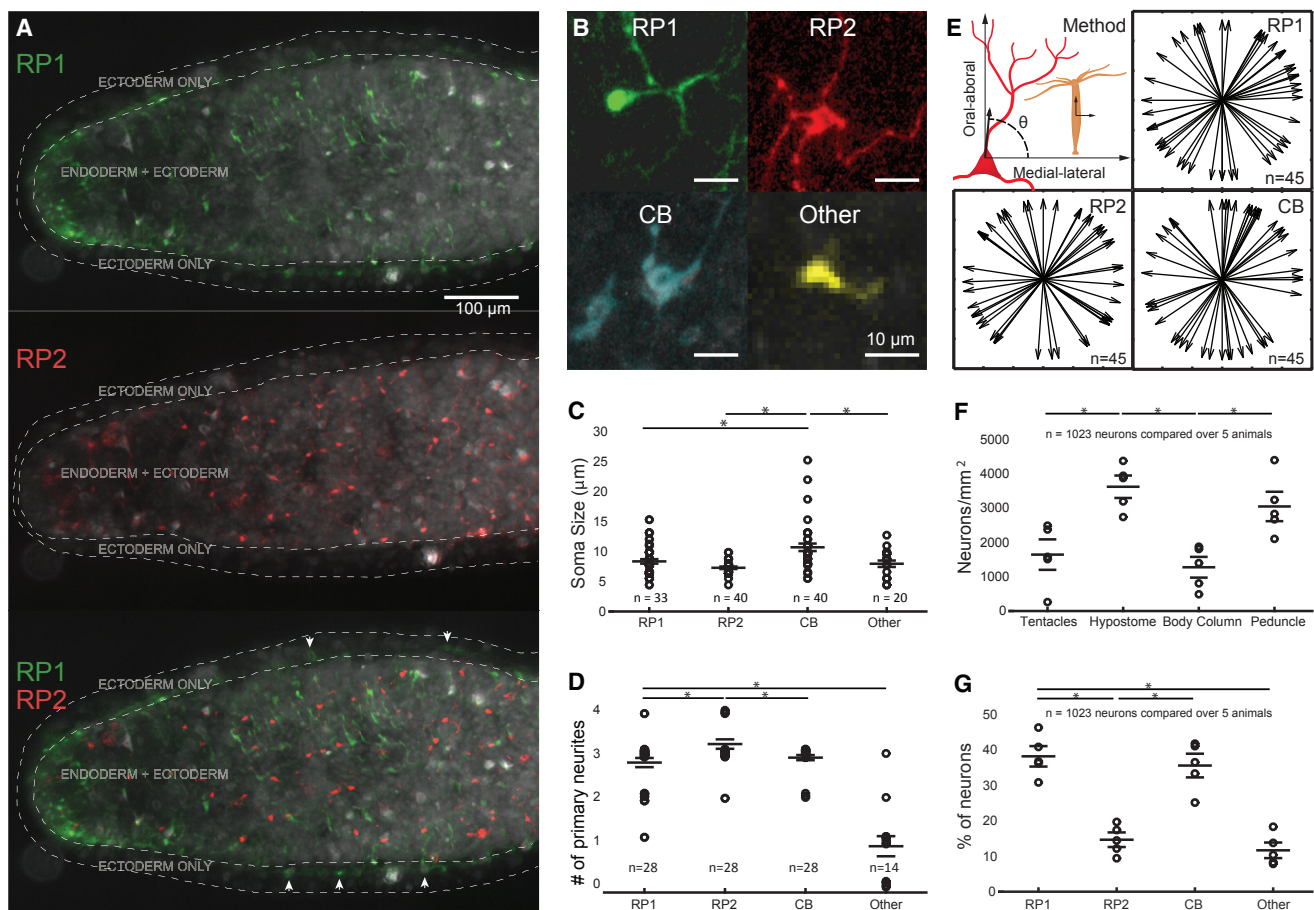


Figure 4. Anatomical Differences between the Three Major Networks

(A) Pseudocolored (cf. Experimental Procedures) RP1 and RP2 networks in an animal's body column. Top: RP1 only. Middle: RP2 only. Bottom: RP1 and RP2. Areas containing the ectoderm only and the endoderm + ectoderm are delineated with white dashed lines, and five example neurons present in the "ectoderm only" areas are marked with arrows.

(B) Pseudocolored neurons representative of each of the four main categories.

(C) Soma size.

(D) Number of primary neurites. Note that jitter was added to the data points so that they do not overlap exactly on the plot.

(E) Orientation of primary neurites in neurons of the three main networks. The method to measure the angle at each neurite is described in the top-left panel.

(F) Neuron density in various body areas.

(G) Percentage of neurons belonging to each network.

Data are represented as mean \pm SEM. *p < 0.05 (unpaired t test). See also Figure S3.

involved a large proportion of the neurons in the animal ($36.8\% \pm 1.87\%$ and $37.1\% \pm 1.6\%$, respectively), as compared with RP2 ($16\% \pm 2\%$) and single other cells ($9.93\% \pm 1.17\%$) ($p < 0.05$, paired t test; Figure 4G). This quantification also supports that RP2 is generated by the endodermal nerve net, because previous studies [5] showed a 1/5 ratio (20%) between endodermal and ectodermal neurons, which is similar to the ratio we found (22%) between the number of neurons participating in RP2 as compared with the sum of neurons in the RP1 and CB networks (see Figure S3). Additionally, this quantification supports our earlier claim that the other neurons are probably sensory cells, because previous studies [3] also reported a very small proportion of sensory cells, as compared with ganglion cells.

Taken together, our data indicate that CB and RP1 networks are composed of two independent sets of ectodermal neurons,

whereas the RP2 network is endodermal. Cells that are not part of these networks are likely to be sensory neurons.

RP1 Is Associated with Elongations and RP2 with Radial Contractions

We then examined whether the activity of these non-overlapping networks correlated with any behavior. As stated, CB activity was clearly associated with the longitudinal CBs of the animal. Also, because RPs were thought to be in the endodermal nerve net, their activation should cause contraction of endodermal muscles and elongation of the body in response to a photic stimulus. For these reasons, because we found that RP1 is ectodermal, we hypothesized that the RP circuit mediating photic response was RP2. To test this, we measured the activity of the nervous system of *Hydra* following photic stimulation. We

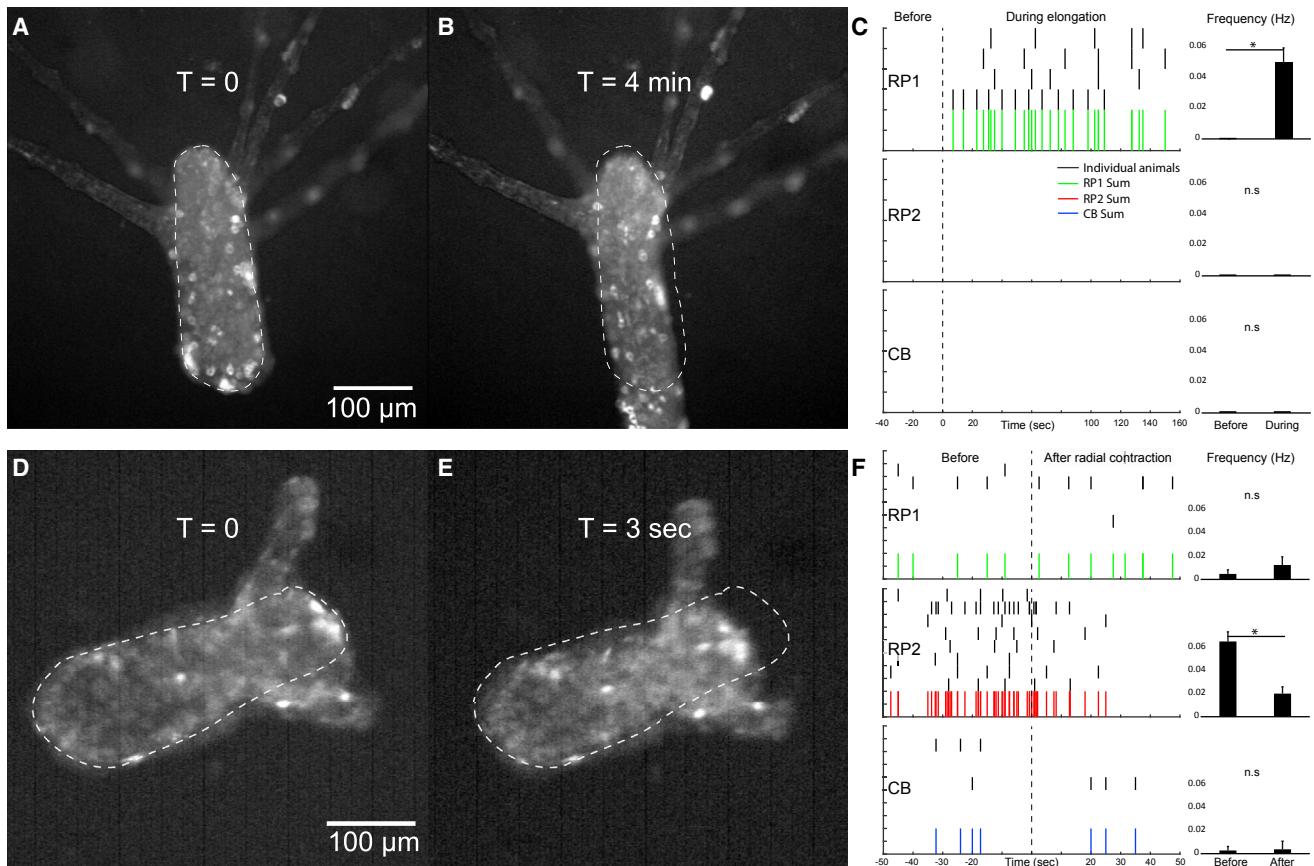


Figure 5. Behavioral Association of Two RP Networks

- (A) Dark-habituuated animal at rest.
- (B) Elongation response during exposure to blue light (see Movie S3). Dashed line marks the body contour of the animal at rest.
- (C) Spike trains of RP1, RP2, and CB neurons in four animals, where t = 0 indicates onset of elongation. Histograms compare firing frequency before versus during elongation response.
- (D) Animal before radial contraction, a behavior that also occurs in unrestrained preparations (Movie S5).
- (E) Animal after radial contraction (see Movie S4). Dashed line marks the body contour of animal before radial contraction.
- (F) Spike trains of RP1, RP2, and CB neurons in eight animals, where t = 0 indicates radial contraction. Histograms compare firing frequency before versus after radial contraction.

Data are represented as mean \pm SEM. *p < 0.05 (paired t test); ns, not significant. See also Movies S3, S4, and S5.

induced light response by first dark-habituating animals overnight under dim infra-red light (Figure 5A). When we switched to fluorescence imaging, the light emitted by the arc lamp caused photic stimulation, which resulted in elongation response (Figure 5B, where a dashed line marks the contour of the animal before elongation; Movie S3). To our surprise, although all three networks were mostly silent during at least 40 s before elongation onset, only RP1, and not RP2, became active after elongation onset (Figure 5C). Therefore, we concluded that RP1, rather than RP2, is correlated with elongations. This is consistent with the fact that neurons of the tentacles are connected to photosensors [30, 38] and RP2 is not present in the tentacles (Figure 3A). Also, the fact that RP1 neurons cause elongation and CB neurons cause longitudinal contraction is consistent with the anti-correlation that we observed between them (Figure 3D) and hints at a push-pull mechanism where the morphology of the animal results from a combination of the activity of two opposed neural ectodermal

networks. It is important to note that, as observed previously [6], the RP1 network is also active independent of the elongation response to light, which suggests that it might be correlated with other behaviors.

We then turned our attention to the functional role of RP2. To our surprise, we discovered that radial contraction was also linked to a change in the frequency of RPs, but that this change was specific to RP2. The slow radial contraction behavior was readily noticed in our time-lapse movies, if we played them at various speeds to recognize changes in animal morphology that happen at slower timescales (Figures 5D and 5E; see also Movie S4). Indeed, the frequency of RP2 decreased significantly after radial contraction ($p < 0.012$, paired t test), whereas the activity of the other networks did not change. Additionally, the frequency of RP2 was on average ten times higher than RP1 and CB, which indicates a particularly high level of excitation before radial contraction. Therefore, we concluded that RP2 participates in radial contraction. This is consistent with the fact that

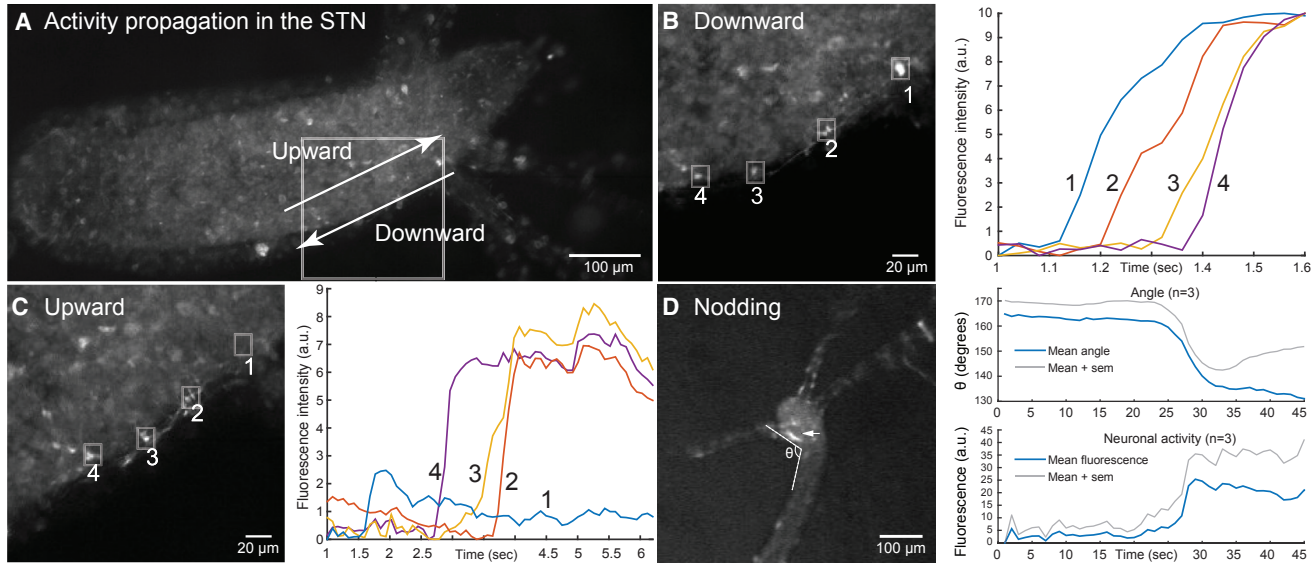


Figure 6. Subtentacle Network Causes Nodding Behavior and Can Conduct Signal in Both Directions

(A) Representative *Hydra*. The white square marks the area containing a subtentacle network (STN). Arrows mark the two directions of propagation: upward and downward.
 (B) Left: region boxed in (A) during downward propagation, with four neurons marked with white squares. Right: calcium trace of the four neurons during downward propagation.
 (C) Same as (B) but for upward propagation.
 (D) Left: representative *Hydra* at the end of nodding. θ marks the angle; the arrow marks one STN neuron. Right: evolution of angle and STN neuronal activity over time.

RP2 is located in the endoderm (Figure 4A), and that endodermal neurons are connected to sensory cells that are exposed to the gastric environment [3]. In this context, RP2 neurons could act as an integrator of information about the gastric environment, which would put them in a position to decide when radial contraction has to occur. If we consider the body column of *Hydra* as a cylinder, the relaxation of the ectodermal longitudinal fibers by RP1 during elongation would change its length, whereas the activation of the endodermal circular fibers by RP2 during radial contraction would change its diameter.

Thus, we concluded that the three networks are involved in three different behaviors selectively: the longitudinal CBs are correlated with the activity of CB, the elongation response to light with RP1, and the radial contraction with RP2. Thus, rather than acting as a single network, the nerve net of *Hydra* creates different behaviors by using anatomically separate networks of neurons.

Subtentacle Network Is Associated with Nodding

Besides the three animal-wide networks (CB, RP1, and RP2), where synchronous activation of neurons occurred throughout the body of the animal, we also observed local activation of neurons in some experiments. In particular, there was one local network that did not belong to RP1, RP2, or CB and that was correlated with nodding behavior, i.e., gentle swaying of the hypostome of the animal and its tentacles to one side but without turning the rest of the body. This network was located just under the tentacles, and we decided to call it the subtentacle network (STN). Specifically, the STN was located at the junction between the tentacle and the body column (Figure 6A). In the STN, cal-

cium signal could propagate downward (Figure 6B) but also upward (Figure 6C). Note that in the example shown in Figure 6, neuron 1 is only activated when the signal propagates downward, which indicates that the activation of the STN circuit does not always recruit all of its neurons. The propagation speed of the calcium signal was $251 \pm 54.6 \mu\text{m/s}$ (SEM, $n = 5$).

The behavioral correlation of the STN with nodding was robust: when activated, the animal always nodded (four out of four animals). To quantify this, we measured the angle formed between the hypostome and the body column (Figure 6D, left) as the fluorescence of the STN neurons changes and observed that the hypostome of the animal starts nodding at the same time as the neurons get activated (Figure 6D, right). We did not notice any difference in nodding when the activation was upward or downward.

Neuronal Activity Can Propagate in Two Directions and at Two Different Speeds in Tentacles

In addition to the STN, we found another example of a local activation of neurons in the tentacles, where propagation can be bidirectional and occur at multiple propagation speeds. Specifically, in the tentacles of four animals, we detected calcium signal that propagates slowly, enabling us to determine the exact direction of propagation of activity. We observed that activity could flow upward or downward (Figure 7, first part of the traces) and, interestingly, in both cases slow propagation was followed by coactivation of all regions of interest (Figure 7, second part of the traces). The average speed of the slow-propagating activity was $63 \pm 30 \mu\text{m/s}$ (SEM, $n = 4$), whereas during coactivation, the speed of signal propagation could not be measured at our

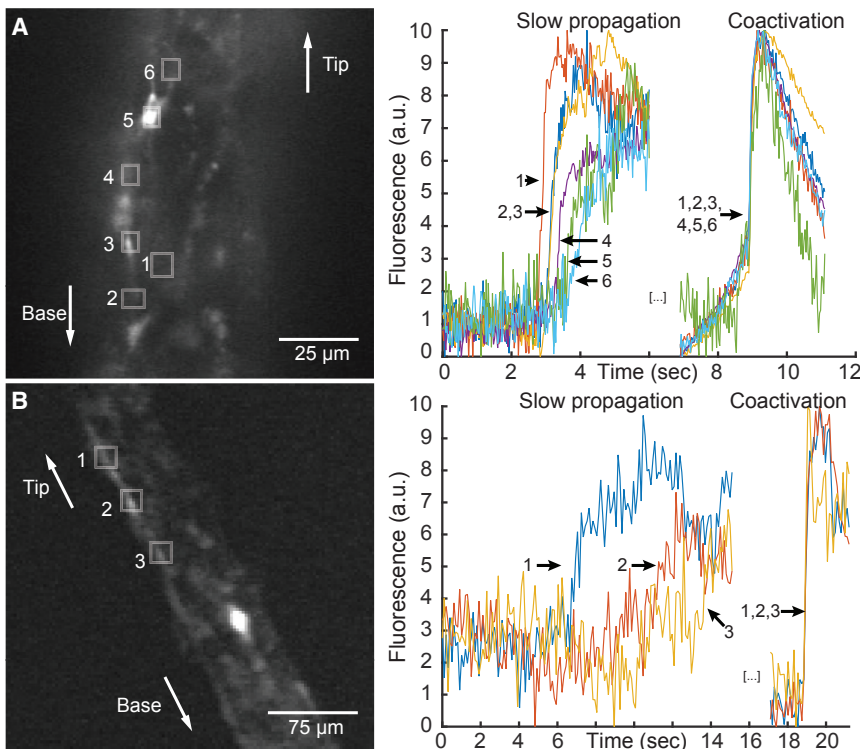


Figure 7. Signal Propagates in Both Directions and at Two Different Speeds in Tentacles

(A) Left: representative tentacle during upward propagation, with six example neurons boxed and numbered in white. Right: calcium signal of the six neurons during slow propagation and coactivation. (B) Same as (A) but for downward propagation.

brafish [48–53]. Work on these species could provide critical insights relevant to understanding the function of the nervous system of mammals and humans.

Here we introduce *Hydra* as an alternative for large-scale measurements of neural activity and to capture and investigate the emergent properties of neural systems. The choice of each animal model has pluses and minuses. Although one cannot apply to *Hydra* traditional genetic tools, through the recent sequencing of its genome [22] and the development of successful transgenesis [24] one can have access to many of the modern molecular approaches standard in other fields of neuroscience. Also, as a preparation, *Hydra* offers some significant advantages

resolution of 33 Hz (here on a field of view of $130 \times 130 \mu\text{m}$). This speed was therefore higher than 7 mm/s, consistent with previous electrophysiological measurements that indicated 4.6 cm/s [9]. However, because we cannot measure the speed of this signal propagation, it is possible that these different regions of interest are not activated in the same sequence and instead are activated in a random fashion. In 3 out of 4 observations, the neurons mediating slow propagation and coactivation were also part of the CB network, and coactivation corresponded to a longitudinal CB.

DISCUSSION

Hydra as a Novel Preparation for Whole-Nervous-System Imaging

As opposed to conventional electrical circuits, the brain is made of neurons that receive and send connections to a large number of other neurons in many different regions at the same time. This organization appears ideal for the generation of emergent functional properties, built with the aggregate spatiotemporal activity of a large number of cells, and these emergent functional states, such as attractors, could be used to implement memories and many computations [39, 40].

To capture these emergent states of function, it seems ideal to be able to measure “every spike from every neuron” and build a “Brain Activity Map” [41], as a step toward deciphering the role of these emergent states in the function of the nervous system or in the generation of behavior or internal brain states. In this regard, whole-brain imaging methods have recently been successful in measuring the activity of large numbers of neurons in animal models such as the worm [42–45], fruit fly [46, 47], and ze-

lages for imaging entire nervous systems. First, it is a cnidarian, and thus represents some of the first nervous systems in evolution, which could enable the elucidation of basic principles of neural circuits more easily. Second, *Hydra* can reproduce asexually by budding, enabling the generation of clonal individuals and the examination of the structural and functional generation of a new animal. Third, its nervous system is distributed without any ganglia, and the animal is transparent, so every neuron can be imaged in isolation. Fourth, because the body of *Hydra* is flexible, it is possible to place it between two coverslips separated by $100 \mu\text{m}$ and keep the animal alive for weeks without observing any sign of injury. The behaviors we measured in this study—longitudinal CBs, elongation response to light, and nodding—do occur in *Hydra*’s natural habitat [6, 9, 13, 14]. Because the definition of radial contraction is vague, we verified it by ourselves in an unrestrained preparation (Movie S5). However, in our restrained preparation, these behaviors might be expressed in a different way. Typically, nodding and elongation response to light will only be possible on the plane that is parallel to the coverslips. Also, longitudinal and radial contractions could be somewhat slowed down because of friction of the animal against the coverslips, and the deformation of the body of the animal could be altered. To test this, we measured the duration of both types of contractions and the resulting change in the width of the animal (Figure S4), and did not detect any significant difference between these behaviors in an unrestrained preparation and between two coverslips.

When used with low-magnification objectives, such preparation allows having the entire network of neurons in focus and alleviates the need for scanning multiple planes in z. Therefore, it is possible to observe the activity of the entire nervous system of

Hydra with a higher temporal resolution while keeping a spatial resolution of single neurons. These advantages make it easier to measure single calcium transients in a behaving animal and attribute them correctly to the neurons that generated them, getting to the ideal of measuring every spike from every neuron [41]. In fact, using immunocytochemistry, we estimate that we are indeed recording the activity of essentially every neuron in the animal. Moreover, at least for many neurons, we are most likely also imaging individual calcium transients.

As an animal model for circuit neuroscience, *Hydra* is amenable to imaging and offers a small repertoire of behaviors to study. We presented the activity of the nervous system during longitudinal CBs, elongation response to light, radial contraction, and nodding, but other behaviors exist, such as somersaulting and feeding. Both of these behaviors add another layer of complexity, because they happen in multiple steps, which requires coordination of activity across the entire animal. For instance, feeding behavior engages first a concerted motion of the tentacles, after which the prey is brought to the mouth in order to be swallowed and digested through peristaltic motion of the body column. Therefore, imaging *Hydra* during these behaviors would help explore coordination of activity across different parts of its nervous system.

Non-overlapping Coactive Networks of Neurons in the Nerve Nets of *Hydra*

Using calcium imaging, we perform the first functional measurements of neurons in *Hydra* and can associate previously recorded electrical signals such as RPs and CBs to specific populations of neurons. Also, a striking feature of the RP1, RP2, and CB networks is the fact that their neurons are coactive (they fire simultaneously or at least within 100 ms). We are still ignorant about the exact connectivity of these neurons, and the joint activity could be the result of either gap junctions connecting every neuron, strong chemical synapses that have a very low failure rate, or inputs from another circuit that is connected to every neuron of this network. Indeed, both chemical synapses and gap junctions have been found in *Hydra* [54, 55], but a third circuit mediating coactivation seems less likely, because we do not observe activity of any other circuit that is simultaneous to RP1, RP2, or CB.

However, regardless of the exact mechanisms of coactivation, we have discovered that the nervous system of *Hydra* is divided into networks that are non-overlapping structurally and functionally, i.e., where individual neurons participate selectively in specific networks and no neuron belongs to more than one network. Moreover, these networks (CB, RP1, RP2, and STN) are associated with specific behaviors of the animal (longitudinal contractions, elongation, radial contraction, and nodding, respectively). As mentioned above, most neurotransmitters can be found in the *Hydra* genome, so there could be a molecular identification of the networks of neurons we identified functionally.

The finding of non-overlapping networks indicates that the nervous system of *Hydra*, and perhaps other cnidarians, is not a single nerve net but is built out of distinct networks whose activity can be linked to specific behaviors. Thus, evolution has carved out a behavioral repertoire by selectively linking subsets of neurons out of a tapestry of apparently similar cells, as each subset of neurons is associated with a specific behavior. This

carving could occur by selectively connecting neurons into subcircuits, or by modifying synaptic strengths. Future work combining connectomics with functional imaging could examine these mechanisms of functional specificity.

Two RP Networks

The use of whole-brain calcium imaging has also allowed us to identify two networks associated with RPs, previously described as a single one using extracellular recordings [14]. These two networks (RP1 and RP2) are located in the ectoderm and endoderm of the animal, respectively. A previous study reported that RPs are only generated in the endoderm [10], by showing their absence in an area where the endoderm had been surgically removed. However, in that study, the authors reported having recorded in rare instances RPs in the ectoderm but they attributed this signal to an incomplete removal of the endoderm in the recorded region. According to our present results, it is likely that in most cases the authors recorded the endodermal RP2 signal and in rare instances they recorded the ectodermal RP1 signal. Also, our report that contraction of the endoderm causes radial contraction is in apparent contradiction with the report that RPs could cause contraction of the endoderm [12]. Indeed, because a change in the frequency of RPs was observed during elongation response [6], it was concluded that contraction of endodermal cells would cause elongation of the animal. However, based on our data, we suggest that the contractions observed by [12] originated in the endodermal RP2 system, which is correlated with radial contraction, whereas the response to light in [6] arose from the ectodermal RP1, which is correlated with elongation.

Interestingly, although RP1 and RP2 are associated with elongation and radial contraction, respectively, because changes in their frequency of activation were clearly associated with behavior, there was no clear-cut temporal correspondence between the activity of RP1 and elongation or between the activation of RP2 and radial contraction (Figure 5). Thus, we hypothesize that, rather than directly triggering or controlling behavior, these two RP networks may integrate sensory information, which then subsequently triggers the behavioral response, through a different cellular element, perhaps even through epithelial cells.

Bidirectional Propagation in the Subtentacle Network

Slow potentials that occur simultaneously with asymmetric longitudinal contraction of the body column were reported in [6]. However, in those experiments, it was not possible to prove or exclude the participation of neurons. Here, we describe the activity of a specific network of neurons (the STN) that are located under the base of the tentacles and that are activated during such behavior.

The sequence of activation of the STN can either initiate in the body column and travel toward the tentacles, or initiate in the tentacle-hypostome junction and travel downward. This flexibility could have a role, such as fine-tuning the resulting motor output by changing which part of the body should bend first. Also, it may have no specific function but arise from the fact that the STN can be activated by different neurons. Indeed, it is possible that activity in the body column and in the hypostome can initiate STN activity. Then, depending on which one

happens, the STN will start either at the hypostome-tentacle junction or in the body column.

Multiple Conduction Speeds

The existence of multiple conduction speeds within the same network has been described in other hydrozoans such as *Aequorea* [18] (p. 482) and anthozoans such as *Calliactis* [56]. For instance, in the hydrozoan *Aequorea*, the radial conduction system is slow (0.002–0.02 m/s, i.e., 2–20 mm/s) whereas the swimming beat system is much faster (0.9 m/s). In our experiments, we observed that in the tentacles of *Hydra* there are calcium transients that travel at $63 \pm 30 \mu\text{m/s}$ (SEM, $n = 4$) and others that might travel at more than 7 mm/s, which differ by two orders of magnitude. As mentioned above, the neurons where slow and fast propagation was observed are most of the time part of CBs, and it is only during fast propagation that longitudinal contraction occurred. Therefore, slow propagation could be the result of a different type of activity that is initiated in one neuron and travels to its neighbors. Such activity could increase the excitability of ganglion and sensory neurons, but could even affect the sensory structures such as nematocytes to which they are connected. In this regard, measuring calcium transients in nematocytes would provide valuable information for studying their interactions with neurons.

Broader Relevance to Neuroscience

The findings presented here may extend to understanding the structure and function of the nervous systems of other cnidarians and basal metazoans. The electrical activity and behaviors of other polyps and medusae have been studied before [18], and many similarities are shared among animals of this phylum. Such similarities include the existence of nerve nets, the spontaneous longitudinal contractions, and the characteristic sequence in feeding behavior. Accordingly, the presence of two networks in the ectodermal nerve net and one network in the endodermal nerve net could be a general feature of the polyp form of cnidarians. From a different perspective, one could take advantage of the subtle differences between polyps of different species, which change in size, shape, and the type of prey they feed on. In such comparative studies, one could test the role of a specific feature of the anatomy, electrical activity, and behavior in an animal where most of the other parameters are essentially the same.

In addition to the interest in the neurobiology of basal metazoans, studies of the nervous system of *Hydra* could have relevance for understanding neural circuits in bilaterian species. Indeed, coordinated spontaneous activity, robustly present in *Hydra*, is common to all nervous systems observed, including mammalian visual cortex [57] and human electroencephalograms. Additionally, it has been proposed that brain waves have evolved from an early form of spontaneous activity such as the one observed in *Hydra* [58]. Also, our finding that the activity of the endodermal nerve net is correlated with the activity of the gastric cavity (radial contraction; Figures 5D–5F) is reminiscent of the enteric nervous system controlling the gastro-intestinal tract of higher animals. More generally, the study of simpler organisms could enable us to discern some basic principles such as emergent properties of neural circuits, analyze the anatomical, biophysical, and synaptic mechanisms that generate them, and understand how they relate to behavior or internal brain states.

EXPERIMENTAL PROCEDURES

Hydra Maintenance

Hydra were maintained in the dark at 18°C and fed freshly hatched *Artemia* nauplii once a week or more frequently when necessary.

Transgenics

Transgenic lines were created according to Juliano et al. [29] using a modified version of the pHyVec1 plasmid (Addgene catalog no. 34789) [28], where we replaced the GFP sequence with a GCaMP6s sequence that was codon-optimized for *Hydra* (DNA2.0). By embryo microinjection one gets mosaic animals, where ectoderm, endoderm, and interstitial lineages can become transgenic separately [59]. We selected animals only expressing GCaMP6s in the interstitial cell lineage. Also, interstitial cell lineage includes neurons, cnidocytes, and gland cells. However, it was possible to discriminate them from neurons in our movies because of their morphological features (only neurons have neurites).

Imaging

In order to record the activity of the nervous system of *Hydra*, we developed a new preparation for functional imaging. Animals were placed between two coverslips that are separated by one 100-μm spacer to keep them on focus. In this preparation, animals might not behave as they would in their natural habitat. However, it makes it convenient to look at the activity of the nervous system of *Hydra* during specific behaviors. Imaging was performed using a fluorescence dissecting microscope (Leica M165) equipped with a long-pass GFP filter set (Leica filter set ET GFP M205FA/M165FC), 1.6× Plan Apo objective, and sCMOS camera (Hamamatsu ORCA-Flash 4.0) or Olympus IX70 inverted microscope equipped with 10× water-immersion objective, U-MIWIB2 GFP filter cube, and an EM-CCD (Hamamatsu EM-CCD C9100-12). In both setups, illumination came from a mercury arc lamp, and the software μManager [60] controlled the microscope. Single neurons were tracked manually, frame by frame, using the graphic user interface of TrackMate [61], and no automated tracking algorithm was ever used (Movie S2). Such single-neuron tracking was only performed to generate Figures 1D and 3B and show that the three circuits of neurons (RP1, RP2, and CB) are mutually exclusive. When a neuron was particularly challenging to track (cf. blue circle in Figure 1D, bottom left), visual landmarks from the surrounding tissue were used as guiding points. For the rest of the manuscript, we only measured at which frame these (RP1, RP2, and CB) networks of neurons fire, which we call “coactivation events” (Figure 1C, right). This is much more straightforward to measure for two reasons. First, whenever any of these circuits is activated, a larger number of neurons fire during the same frame, which makes it easy to detect. Second, each circuit is easily recognizable: activation of CB always results in longitudinal contraction, and RP1, but not RP2, invades the tentacles. Data coming from these measurements were then plotted as a spike train (Figure 1C, right, green bars; Figures 3 and 5), where each spike indicates coactivation of all of the neurons of that circuit. All of the collected data were handled with MATLAB (The MathWorks). The main advantage of this preparation is the fact that there is no need to scan in the z axis, and therefore the acquisition speed is only limited by the camera. The main disadvantage is the fact that by using wide-field imaging rather than confocal or two-photon imaging, the spatial resolution is worse (about 1 μm for wide-field, when compared to less than 0.4 μm for the others). This can result in cross-contamination between regions of interest and, for instance, in the increase in fluorescence of some RP1 neurons during a CB event because of light scattering coming from CB neurons lying in close proximity to the recorded RP1 neuron (e.g., in Figure 2C). This cross-contamination makes it difficult to tell whether a neuron is firing based on fluorescence trace alone. However, it is easy to tell in movies when a neuron is firing, because its neurites are also lighting up. For this reason, the spike times were manually measured in the movies for each neuron.

Pseudocoloring

We used pseudocoloring as a method for identifying neurons that fired during the same frame (e.g., in Figure 4A). For a given firing event, using ImageJ [62], we subtracted the frame before neurons fired from the frame during which neurons fired. We then added the result of this subtraction in a specific color to the frame before neurons fired.

Electrophysiology

Sharp electrodes were pulled from borosilicate glass (Sutter catalog no. BF150-86-10) with a Sutter p-97 pipet puller in order to obtain a resistance of 50–100 MΩ. They were then filled with 3 M KCl and 40 μM Alexa 488. Animals were impaled under visualization with calcium imaging using a similar setup as in the previous experiments, except that the microscope was an upright Olympus BX51WI. Electrical signal was acquired with a MultiClamp 700B (Axon Instruments) and the software PackIO (<http://packio.org>) [63].

Statistical Methods

Statistics are indicated as average ± SEM in figures and in the text. Cross-correlation was computed between spike trains using the MATLAB function xcorr. To compare the number of spikes before versus after radial contraction, we ran a two-tailed paired t test assuming equal variance using Microsoft Excel. To compare morphological parameters, we used two-tailed, paired, or unpaired Student's t tests as specified in the text.

SUPPLEMENTAL INFORMATION

Supplemental Information includes Supplemental Experimental Procedures, four figures, and five movies and can be found with this article online at <http://dx.doi.org/10.1016/j.cub.2017.02.049>.

AUTHOR CONTRIBUTIONS

Conceptualization, C.D. and R.Y.; Methodology, C.D. and R.Y.; Investigation, C.D.; Writing – Original Draft, C.D.; Writing – Review & Editing, C.D. and R.Y.; Funding Acquisition, R.Y.; Resources, C.D. and R.Y.

ACKNOWLEDGMENTS

We thank Sydney Brenner for advice and the suggestion to work on *Hydra*; Charles David, Rob Steele, Celina Juliano, Shuting Han, and John Szymanski for technical help and comments; Kaniz Fatema, Stephen Leong, and Sanjana Salwi for help with neuron tracking; and Mac Passano and George Mackie for their correspondence. This work was supported by NIH Pioneer award DP1EY024503 (to R.Y.). This material is based upon work supported by the Defense Advanced Research Projects Agency (DARPA) under contract no. HR0011-17-C-0026 and the US Army Research Laboratory and the US Army Research Office (contract W911NF-12-1-0594; MURI).

Received: August 21, 2016

Revised: November 8, 2016

Accepted: February 20, 2017

Published: March 30, 2017

REFERENCES

1. van Leeuwenhoek, A. (1702). Part of a letter from Mr Antony van Leeuwenhoek, F. R. S. concerning green weeds growing in water, and some animalcula found about them. *Philos. Trans.* 23, 1304–1311.
2. David, C.N. (1973). A quantitative method for maceration of *Hydra* tissue. *Arch. Entwicklmech. Org.* 171, 259–268.
3. Westfall, J.A., Wilson, J.D., Rogers, R.A., and Kinnamon, J.C. (1991). Multifunctional features of a gastrodermal sensory cell in *Hydra*: three-dimensional study. *J. Neurocytol.* 20, 251–261.
4. Parker, G.H. (1919). The Elementary Nervous System (J.B. Lippincott).
5. Epp, L., and Tardent, P. (1978). The distribution of nerve cells in *Hydra attenuata* Pall. *Roux Arch. Dev. Biol.* 185, 185–193.
6. Passano, L.M., and McCullough, C.B. (1962). The light response and the rhythmic potentials of *Hydra*. *Proc. Natl. Acad. Sci. USA* 48, 1376–1382.
7. Rushforth, N.B., and Burke, D.S. (1971). Behavioral and electrophysiological studies of *Hydra*. II. Pacemaker activity of isolated tentacles. *Biol. Bull.* 140, 502–519.
8. Kass-Simon, G. (1972). Longitudinal conduction of contraction burst pulses from hypostomal excitation loci in *Hydra attenuata*. *J. Comp. Physiol.* 80, 29–49.
9. Passano, L.M., and McCullough, C.B. (1965). Co-ordinating systems and behaviour in *Hydra*. II. The rhythmic potential system. *J. Exp. Biol.* 42, 205–231.
10. Kass-Simon, G., and Passano, L.M. (1978). A neuropharmacological analysis of the pacemakers and conducting tissues of *Hydra attenuata*. *J. Comp. Physiol.* 128, 71–79.
11. Kay, J.C., and Kass-Simon, G. (2009). Glutamatergic transmission in *Hydra*: NMDA/D-serine affects the electrical activity of the body and tentacles of *Hydra vulgaris* (Cnidaria, Hydrozoa). *Biol. Bull.* 216, 113–125.
12. Shibley, G. (1969). Gastrodermal contractions correlated with rhythmic potentials and prelocomotor bursts in *Hydra*. *Am. Zool.* 9, 586.
13. Haug, G. (1933). Die Lichtreaktionen der Hydren: *Chlorohydra viridis* und *Pelmatohydra oligactis* (P.) typica. *Z. Vgl. Physiol.* 19, 246–303.
14. Passano, L.M., and McCullough, C.B. (1963). Pacemaker hierarchies controlling the behaviour of *Hydras*. *Nature* 199, 1174–1175.
15. Trembley, A. (1744). Mémoires pour Servir à l'Histoire d'un Genre de Polypes D'eau Douce, à Bras en Forme de Cornes (Jean and Herman Verbeek).
16. Ewer, R.F. (1947). On the functions and mode of action of the nematocysts of *Hydra*. *Proc. Zool. Soc. Lond.* 117, 365–376.
17. Lasker, H.R., Syron, J.A., and Clayton, W.S., Jr. (1982). The feeding response of *Hydra viridis*: effects of prey density on capture rates. *Biol. Bull.* 162, 290–298.
18. Bullock, T.H., and Horridge, G.A. (1965). Structure and Function in the Nervous System of Invertebrates (W.H. Freeman).
19. Kass-Simon, G., and Diesl, V.K. (1977). Spontaneous and evoked potentials from dissociated epithelial cells of *Hydra*. *Nature* 265, 75–77.
20. Campbell, R.D., Josephson, R.K., Schwab, W.E., and Rushforth, N.B. (1976). Excitability of nerve-free *Hydra*. *Nature* 262, 388–390.
21. Ruggieri, R.D., Pierobon, P., and Kass-Simon, G. (2004). Pacemaker activity in *Hydra* is modulated by glycine receptor ligands. *Comp. Biochem. Physiol. A Mol. Integr. Physiol.* 138, 193–202.
22. Chapman, J.A., Kirkness, E.F., Simakov, O., Hampson, S.E., Mitros, T., Weimaiyer, T., Rattei, T., Balasubramanian, P.G., Borman, J., Busam, D., et al. (2010). The dynamic genome of *Hydra*. *Nature* 464, 592–596.
23. Sakarya, O., Armstrong, K.A., Adamska, M., Adamski, M., Wang, I.F., Tidor, B., Degnan, B.M., Oakley, T.H., and Kosik, K.S. (2007). A post-synaptic scaffold at the origin of the animal kingdom. *PLoS ONE* 2, e506.
24. Wittlieb, J., Khalturin, K., Lohmann, J.U., Anton-Erxleben, F., and Bosch, T.C.G. (2006). Transgenic *Hydra* allow *in vivo* tracking of individual stem cells during morphogenesis. *Proc. Natl. Acad. Sci. USA* 103, 6208–6211.
25. Yuste, R., and Katz, L.C. (1991). Control of postsynaptic Ca²⁺ influx in developing neocortex by excitatory and inhibitory neurotransmitters. *Neuron* 6, 333–344.
26. Martínez, D.E. (1998). Mortality patterns suggest lack of senescence in *Hydra*. *Exp. Gerontol.* 33, 217–225.
27. Layden, M.J., Rentzsch, F., and Röttinger, E. (2016). The rise of the starlet sea anemone *Nematostella vectensis* as a model system to investigate development and regeneration. *Wiley Interdiscip. Rev. Dev. Biol.* 5, 408–428.
28. Dana, C.E., Glauber, K.M., Chan, T.A., Bridge, D.M., and Steele, R.E. (2012). Incorporation of a horizontally transferred gene into an operon during cnidarian evolution. *PLoS ONE* 7, e31643.
29. Juliano, C.E., Lin, H., and Steele, R.E. (2014). Generation of transgenic *Hydra* by embryo microinjection. *J. Vis. Exp.* 91, 51888.
30. Plachetzki, D.C., Fong, C.R., and Oakley, T.H. (2012). Cnidocyte discharge is regulated by light and opsin-mediated phototransduction. *BMC Biol.* 10, 17.

31. Passano, L.M., and McCullough, C.B. (1964). Co-ordinating systems and behaviour in *Hydra*. I. Pacemaker system of the periodic contractions. *J. Exp. Biol.* 41, 643–664.
32. Hufnagel, L., and Kass-Simon, G. (1976). The ultrastructural basis for the electrical coordination between epithelia of *Hydra*. In *Coelenterate Ecology and Behavior*, G.O. Mackie, ed. (Springer), pp. 695–704.
33. Tardent, P., and Weber, C. (1976). A qualitative and quantitative inventory of nervous cells in *Hydra attenuata* Pall. In *Coelenterate Ecology and Behavior*, G.O. Mackie, ed. (Springer), pp. 501–502.
34. Hansen, G.N., Williamson, M., and Grimmelikhuijen, C.J.P. (2002). A new case of neuropeptide coexpression (RGamide and LWamides) in *Hydra*, found by whole-mount, two-color double-labeling *in situ* hybridization. *Cell Tissue Res.* 308, 157–165.
35. Hansen, G.N., Williamson, M., and Grimmelikhuijen, C.J.P. (2000). Two-color double-labeling *in situ* hybridization of whole-mount *Hydra* using RNA probes for five different *Hydra* neuropeptide preprohormones: evidence for colocalization. *Cell Tissue Res.* 301, 245–253.
36. Koizumi, O., Itazawa, M., Mizumoto, H., Minobe, S., Javois, L.C., Grimmelikhuijen, C.J., and Bode, H.R. (1992). Nerve ring of the hypostome in *Hydra*. I. Its structure, development, and maintenance. *J. Comp. Neurol.* 326, 7–21.
37. Yum, S., Takahashi, T., Koizumi, O., Ariura, Y., Kobayakawa, Y., Mohri, S., and Fujisawa, T. (1998). A novel neuropeptide, Hym-176, induces contraction of the ectodermal muscle in *Hydra*. *Biochem. Biophys. Res. Commun.* 248, 584–590.
38. Guertin, S., and Kass-Simon, G. (2015). Extraocular spectral photosensitivity in the tentacles of *Hydra vulgaris*. *Comp. Biochem. Physiol. A Mol. Integr. Physiol.* 184, 163–170.
39. Hopfield, J.J. (1982). Neural networks and physical systems with emergent collective computational abilities. *Proc. Natl. Acad. Sci. USA* 79, 2554–2558.
40. Hopfield, J.J., and Tank, D.W. (1985). “Neural” computation of decisions in optimization problems. *Biol. Cybern.* 52, 141–152.
41. Alivisatos, A.P., Chun, M., Church, G.M., Greenspan, R.J., Roukes, M.L., and Yuste, R. (2012). The Brain Activity Map Project and the challenge of functional connectomics. *Neuron* 74, 970–974.
42. Venkatachalam, V., Ji, N., Wang, X., Clark, C., Mitchell, J.K., Klein, M., Tabone, C.J., Florman, J., Ji, H., Greenwood, J., et al. (2016). Pan-neuronal imaging in roaming *Caenorhabditis elegans*. *Proc. Natl. Acad. Sci. USA* 113, E1082–E1088.
43. Nguyen, J.P., Shipley, F.B., Linder, A.N., Plummer, G.S., Liu, M., Setru, S.U., Shaevitz, J.W., and Leifer, A.M. (2016). Whole-brain calcium imaging with cellular resolution in freely behaving *Caenorhabditis elegans*. *Proc. Natl. Acad. Sci. USA* 113, E1074–E1081.
44. Prevedel, R., Yoon, Y.-G., Hoffmann, M., Pak, N., Wetzstein, G., Kato, S., Schrödel, T., Raskar, R., Zimmer, M., Boyden, E.S., and Vaziri, A. (2014). Simultaneous whole-animal 3D imaging of neuronal activity using light-field microscopy. *Nat. Methods* 11, 727–730.
45. Schrödel, T., Prevedel, R., Aumayr, K., Zimmer, M., and Vaziri, A. (2013). Brain-wide 3D imaging of neuronal activity in *Caenorhabditis elegans* with sculpted light. *Nat. Methods* 10, 1013–1020.
46. Chhetri, R.K., Amat, F., Wan, Y., Höckendorf, B., Lemon, W.C., and Keller, P.J. (2015). Whole-animal functional and developmental imaging with isotropic spatial resolution. *Nat. Methods* 12, 1171–1178.
47. Grover, D., Katsuki, T., and Greenspan, R.J. (2016). Flyception: imaging brain activity in freely walking fruit flies. *Nat. Methods* 13, 569–572.
48. Ahrens, M.B., Li, J.M., Orger, M.B., Robson, D.N., Schier, A.F., Engert, F., and Portugues, R. (2012). Brain-wide neuronal dynamics during motor adaptation in zebrafish. *Nature* 485, 471–477.
49. Dunn, T.W., Mu, Y., Narayan, S., Randlett, O., Naumann, E.A., Yang, C.T., Schier, A.F., Freeman, J., Engert, F., and Ahrens, M.B. (2016). Brain-wide mapping of neural activity controlling zebrafish exploratory locomotion. *eLife* 5, e12741.
50. Wolf, S., Supatto, W., Debrégeas, G., Mahou, P., Kruglik, S.G., Sintes, J.-M., Beaurepaire, E., and Candelier, R. (2015). Whole-brain functional imaging with two-photon light-sheet microscopy. *Nat. Methods* 12, 379–380.
51. Panier, T., Romano, S.A., Olive, R., Pietri, T., Sumbre, G., Candelier, R., and Debrégeas, G. (2013). Fast functional imaging of multiple brain regions in intact zebrafish larvae using selective plane illumination microscopy. *Front. Neural Circuits* 7, 65.
52. Portugues, R., Feierstein, C.E., Engert, F., and Orger, M.B. (2014). Whole-brain activity maps reveal stereotyped, distributed networks for visuomotor behavior. *Neuron* 81, 1328–1343.
53. Tomer, R., Lovett-Barron, M., Kauvar, I., Andelman, A., Burns, V.M., Sankaran, S., Grosenick, L., Broxton, M., Yang, S., and Deisseroth, K. (2015). SPED light sheet microscopy: fast mapping of biological system structure and function. *Cell* 163, 1796–1806.
54. Westfall, J.A., Yamataka, S., and Enos, P.D. (1971). Ultrastructural evidence of polarized synapses in the nerve net of *Hydra*. *J. Cell Biol.* 51, 318–323.
55. Westfall, J.A., Kinnamon, J.C., and Sims, D.E. (1980). Neuro-epitheliomuscular cell and neuro-neuronal gap junctions in *Hydra*. *J. Neurocytol.* 9, 725–732.
56. McFarlane, I.D. (1969). Two slow conduction systems in the sea anemone *Calliactis parasitica*. *J. Exp. Biol.* 51, 377–385.
57. Miller, J.-E.K., Ayzenshtat, I., Carrillo-Reid, L., and Yuste, R. (2014). Visual stimuli recruit intrinsically generated cortical ensembles. *Proc. Natl. Acad. Sci. USA* 111, E4053–E4061.
58. Passano, L.M. (1963). Primitive nervous systems. *Proc. Natl. Acad. Sci. USA* 50, 306–313.
59. Khalturin, K., Anton-Erxleben, F., Milde, S., Plötz, C., Wittlieb, J., Hemmrich, G., and Bosch, T.C.G. (2007). Transgenic stem cells in *Hydra* reveal an early evolutionary origin for key elements controlling self-renewal and differentiation. *Dev. Biol.* 309, 32–44.
60. Edelstein, A., Amodaj, N., Hoover, K., Vale, R., and Stuurman, N. (2010). Computer control of microscopes using μ Manager. *Curr. Protoc. Mol. Biol.* 92, 14.20.1–14.20.17.
61. Schindelin, J., Arganda-Carreras, I., Frise, E., Kaynig, V., Longair, M., Pietzsch, T., Preibisch, S., Rueden, C., Saalfeld, S., Schmid, B., et al. (2012). Fiji: an open-source platform for biological-image analysis. *Nat. Methods* 9, 676–682.
62. Schneider, C.A., Rasband, W.S., and Eliceiri, K.W. (2012). NIH Image to ImageJ: 25 years of image analysis. *Nat. Methods* 9, 671–675.
63. Watson, B.O., Yuste, R., and Packer, A.M. (2016). PackIO and EphysViewer: software tools for acquisition and analysis of neuroscience data. *bioRxiv*. <http://dx.doi.org/10.1101/054080>.

Current Biology, Volume 27

Supplemental Information

Non-overlapping Neural Networks in *Hydra vulgaris*

Christophe Dupre and Rafael Yuste

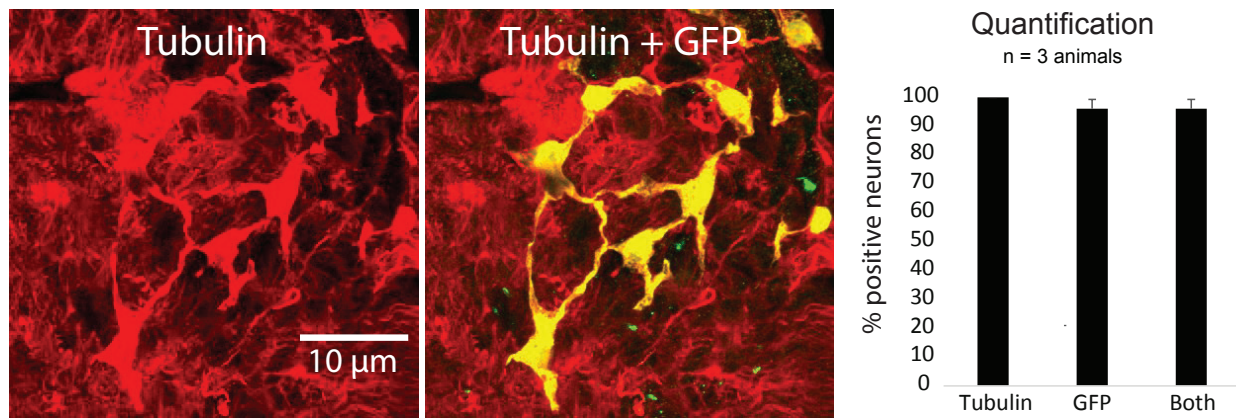


Figure S1. Percentage of transgenic neurons. Related to Figure 1

Left: Immunostaining with acetylated alpha-tubulin antibody only. Middle: Immunostaining with both GCaMP6s and acetylated alpha-tubulin antibodies. Right: Overlap between the two stainings. Error bars indicate SEM.

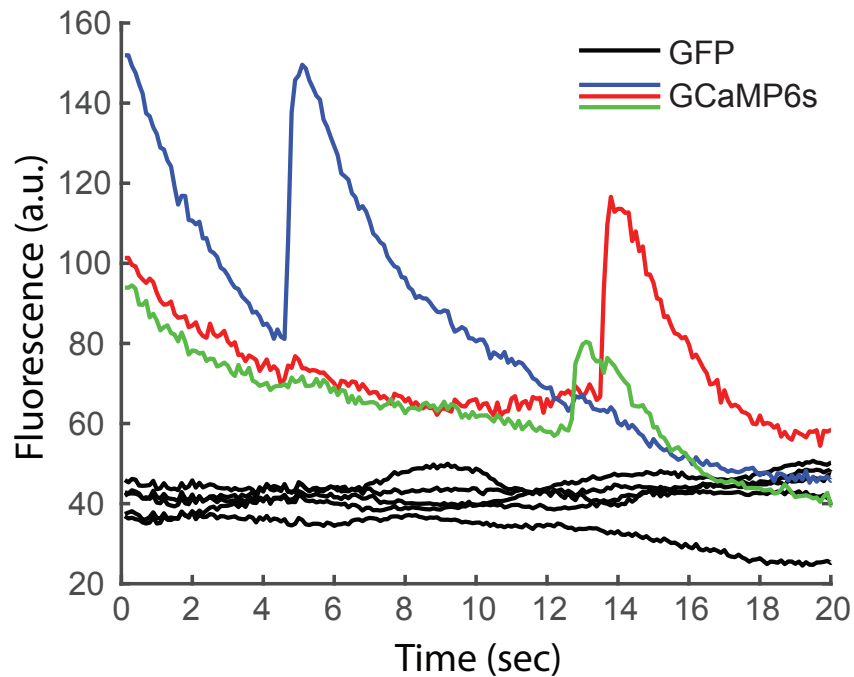


Figure S2. Fluorescence transients in cells expressing GFP compared to GCaMP6s. Related to Figure 1

The green, red and blue traces correspond to neurons expressing GCaMP6s which belong to the RP1, RP2 and CB groups, respectively. The black traces correspond to 5 neurons of another transgenic line expressing GFP in neurons. Both GFP and GCaMP6s signals were recorded during the same behavioral sequence: the last two pulses of a contraction burst, followed by about 15 seconds of elongation.

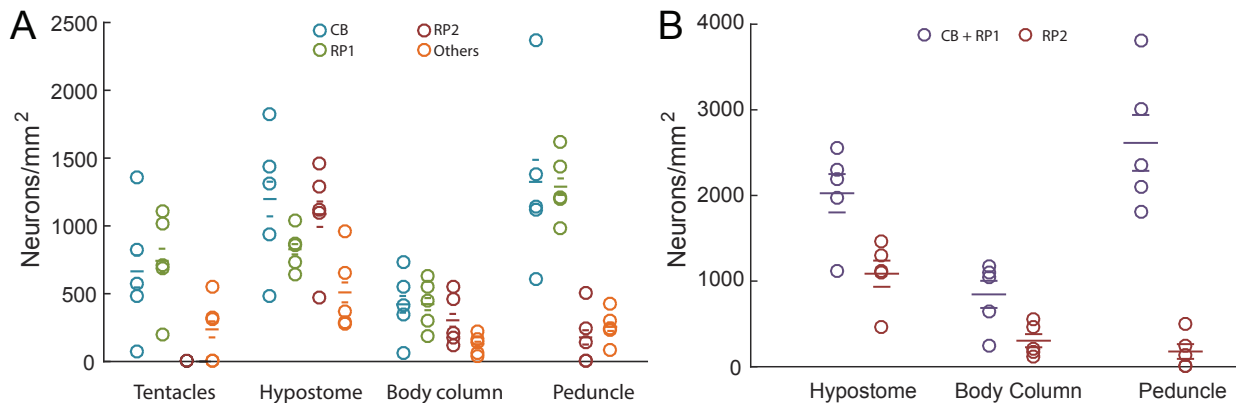


Figure S3. Distribution of neuronal density. Related to Figure 4

Neuronal density in different animal parts, according to each cell type (A) and when RP1 and CB are combined (B). A. The density of RP1 and CB neurons is higher in the hypostome and the peduncle than in the body column. The density of RP2 neurons is not significantly different between the peduncle and the body column, but higher in the hypostome. B. RP1 + CB versus RP2 give density patterns similar to the patterns reported in Epp and Tardent (1978) for ectoderm versus endoderm. $n = 1023$ neurons compared over 5 animals. Wide bars indicate mean, narrow bars indicate SEM.

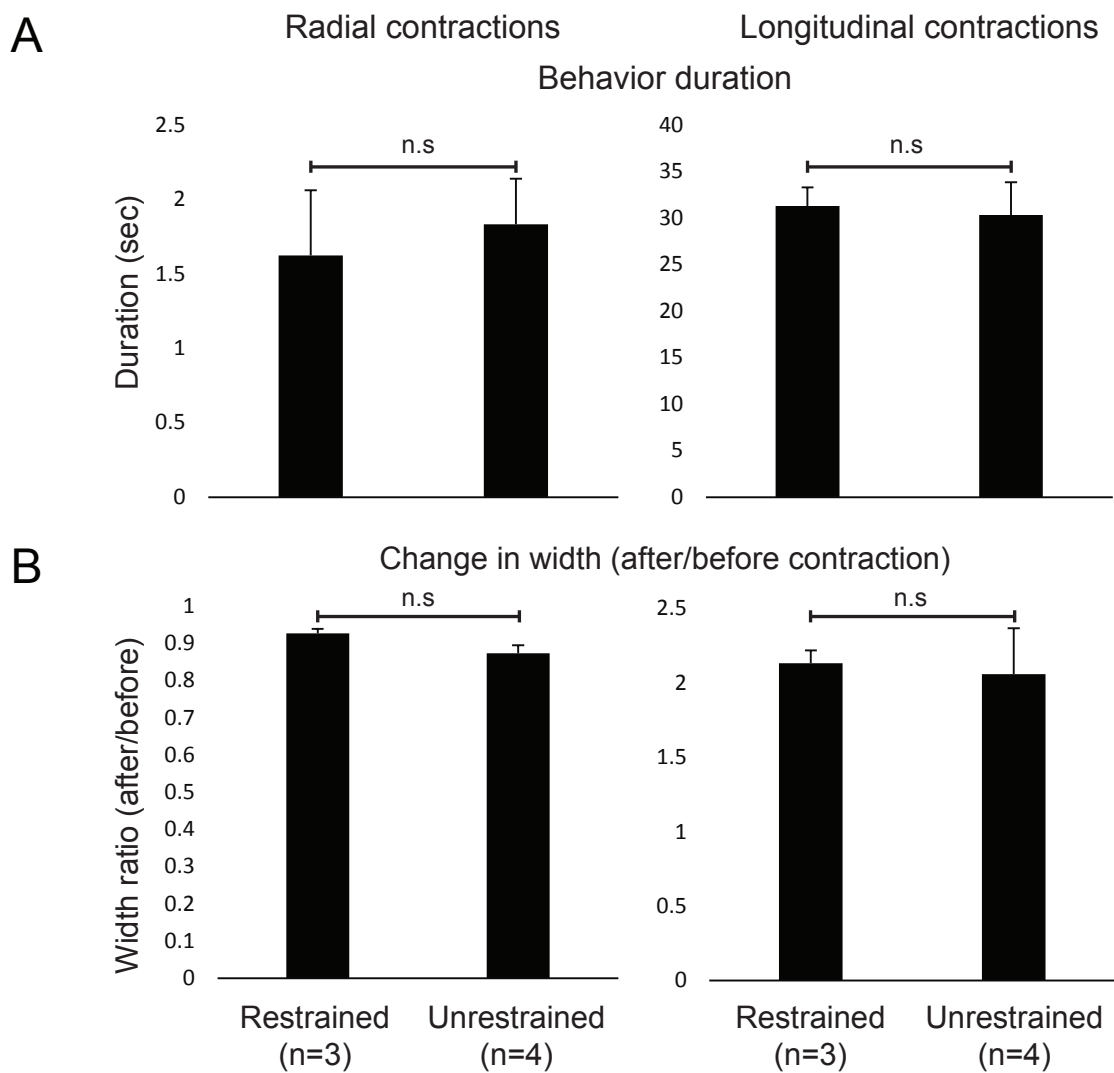


Figure S4. Differences in behavior between restrained and unrestrained preparation. Related to Figure 1

A) Duration of radial and longitudinal contractions in restrained vs unrestrained preparation. B) Change in width of the animal following radial and longitudinal contractions in restrained vs unrestrained preparation. Unpaired T-Test was used, with n.s = not significant ($P > 0.05$).

Supplemental Experimental Procedures

Hydra maintenance

Hydra from AEP strain were maintained in the dark at 18C and were fed freshly hatched artemia nauplii once a week or more frequently when the colony needed to grow.

Transgenics

Transgenic lines were created according to [S1]. Accordingly, *Hydra* oocytes were injected with DNA (2.5 mg/mL) through a micropipet made with a pipet puller (Sutter Instruments model P-97) from borosilicate glass pipets (Sutter instruments, cat# BF100-50-10) and held with a microinjector (Narishige cat#IM-9B) controlled with a joystick micromanipulator (Narishige MN-151).

The DNA that was injected was a modified version of the pHyVec1 plasmid (Addgene cat#34789) [S2] where we replaced the GFP sequence (found between the psrl and EcoRI restriction sites) with a GCaMP6s sequence that was codon-optimized for *Hydra* (DNA2.0, Menlo Park, CA).

Just before the injection, 10 µl of DNA (2.5 mg/mL) were added to 6µl of phenol red and centrifuged for 10 min at max speed to collect debris at the bottom of the tube.

Once the eggs were injected, they were placed in the dark at 18C for 2 weeks and then put back at room temperature on the bench. After a few days, eggs started hatching and the young hatchlings were fed for a couple of days before being screened for transgenic neurons. Transgenic *Hydra* generated this way are mosaic. Therefore, we kept these animals growing and asexually reproducing, and selected the offsprings according to the amount of neurons that were expressing the transgene (a procedure known as clonal propagation). We repeated this procedure until the amount of expression reached a maximum.

Based on this procedure, we expect each transgenic cell to have the same genome since only one injection of the plasmid occurred and that every animal was obtained from the same original individual by asexual reproduction. Also, the expression is driven by an actin promoter for which the use is likely to be similar in different neurons of the same population. It is important to note that the level of expression of the transgene changes dramatically over time. Indeed, it happens frequently that the amount of fluorescence of one animal goes from very high to very low within a few hours. This could be due to the fact that the expression of actin is regulated by factors affecting the entire animal (e.g. hormones) on a slow time scale. Therefore, time-lapse recordings are only performed when the level of fluorescence is high.

Imaging

Animals were placed between two coverslips (VWR cat# 89015-724 and VWR cat#16004-094) that are separated by one 100um spacer (Grace Bio-Labs cat#654006), which allows the animal to move while preventing any part of it from getting out of focus. Imaging was performed using a fluorescence dissecting microscope (Leica M165) equipped with a long-pass GFP filter set (Leica filter set ET GFP M205FA/M165FC) and a sCMOS camera (Hamamatsu ORCA-Flash 4.0) or an Olympus IX-70 inverted microscope equipped with U-MIWIB2 GFP filter cube and an EM-CCD (Hamamatsu EM-CCD C9100-12). In both setups, illumination came from a mercury arc lamp and the software micromanager [S3] controlled the microscope.

Classification of spikes (e.g. RP1, RP2, CB) was made with the help of a home-made MATLAB script that finds fluorescence spikes and displays a snippet of the video that corresponds to that event so that the user can classify each spike as being part of RP1, RP2 or CB.

The images were visualized with Fiji. In order to extract the fluorescence of the neurons, the cells were tracked using TrackMate [S4], and the data was then handled with MATLAB (The Mathworks, Natick, MA). It was not always possible to determine whether the tracked features were cells or swellings, and it is possible that in addition to cell bodies we also tracked such swellings.

Note that in our preparation, *Hydra* were placed between two coverslips and exposed to intense blue light from the arc lamp during imaging. Therefore, the animals were subject to strong tactile and photic stimulation which could affect our data. However, the observed frequency of rhythmic potentials and contraction bursts was similar to what was observed in previous studies where the animal was not restrained [S5,S6]. This indicates that the preparation did not affect the activity of the nervous system to a noticeable level.

Pseudocoloring

Because there is no method to stain neurons according to their functional type (e.g. RP1, RP2, CB), we used pseudocoloring in a few figures in order to label them according to their group. Accordingly, pseudocolored pictures were obtained by subtracting the frame before neurons were activated from the frame during which neurons were activated. The result of this subtraction was then added, in a specific color, to the frame before neurons were

activated. In the resulting picture, the activated neurons showed up in the specific color on a grey background made of all the signal that did not come from the neurons' activation.

Statistics

Cross-correlation

Every spikes of the RP1, RP2 and CB circuit were extracted from the movies and considered as spike trains. Then, cross-correlation was computed between these trains using the MATLAB function xcorr. The time lag used for cross-correlation measurement was 250 seconds.

To compare the number of spikes before vs after egestion, we ran a two-tailed paired T-test assuming equal variance using Microsoft Excel.

Comparison of morphological parameters

We used 2-tailed, paired student T-test. We indicated averages and standard errors on histograms and in the text.

Supplemental plasmid sequence. Related to Figure 1

The pHyVec1 - GCaMP6s plasmid was made by inserting a codon-optimized (DNA2.0, Menlo Park, CA) GCaMP6s sequence between PstI and EcoRI in the pHyVec1 vector. Accordingly, the codon optimized sequence was (fasta format):

>GCaMP6s

```
CTGCAGCCCCGGTAGAAAAAATGGGTAGTCATCACCATCATCACCAACCGGAATGGCATCAATGACAGG  
AGGACAGCAAATGGGCGTGATTTGTATGACGACGATGATAAGATTGGCTACTATGGTGATTCAA  
GCCGCCGTAAATGGAATAAGACTGGTCATGCTGTACGAGCTATTGGAAGGTTAAGTCCCTGAAAAT  
GTTTATATAAAAGCAGATAAGCAGAAAAATGGTATCAAAGCTAATTTCATATACGACATAACATTGA  
AGATGGTGGTGTCAACTTGCATATCACTATCAACAGAACACTCCTATTGGCGACGGACCTGTTTACT  
TCCGTATAATCATTATCTATCTGTCCAATCAAACACTGTCTAAAGACCCAAACGAAAAACGTGATCATA  
TGGTTCTTTGGAATTGTGACGGCTGCCGGTATTACATTAGGGATGGATGAGCTTACAAGGGGGT  
ACCGGTGGTAGTATGGTTTCGAAAGGAGAAGAGAGTTACTGGAGTAGTACCAATTCTGGTTGAATT  
AGACGGAGATGTTAATGGTCATAAATTTCAGTTCTGGAGAAGGGGAAGGAGATGCTACATATGGAA  
AACTTACGCTTAAGTCATATGCACCACAGGAAAATTGCCTGTTCCATGGCCCACCTGGTTACAACAT  
TAACATATGGTGTCCAATGTTTAGTAGATATCCAGATCATATGAAACAACATGACTTTCAAATCTG  
CAATGCCAGAAGGCTATATTCAAGAGAGAACTATATTAAAGGATGATGAAACTATAAGACAAGA  
GCTGAAGTGAATTAGGAGATACTTAGTGAATCGCATAGAACTTAAAGGTATAGACTTTAAAGA  
GGATGGCAATATTAGGTACAAATTAGAGTACAATCTACCTGATCAACTAACAGAGGAACAGATTG  
CAGAGTTCAAAGAGGCATTTCACTTTGATAAAGATGGCGATGGAACAATCACTACTAAGGAATT  
GGTACTGTAATGAGATCACTGGTCAAAACCTACTGAAGCGGAATTACAAGATATGATTAACGAAGT  
AGATGCAGATGGGGATGGAACATAGACTTCCGGAATTAAACATGATGGCACGAAAAATGAAAT  
ACCGTGATACTGAAGAGGAATTAGAGAAGCATTGGTGTATTGACAAAGATGAAACGGTTACATT  
TCTGCTGCTGAACTAAGACATGTTATGACAAACTTAGGAGAAAAACTGACTGATGAAGAGGTCGACG  
AAATGATAAGAGAAGCCGATATTGATGGAGATGGTCAAGTTAACAGAGTTGTTCAAATGATG  
ACAGCAAAGTAAGAATT
```

Supplemental References

- S1. Juliano, C.E. (2014). Generation of Transgenic Hydra by Embryo Microinjection. *J. Vis. Exp.* 91, e51888.
- S2. Dana, C.E., Glauber, K.M., Chan, T.A., Bridge, D.M., and Steele, R.E. (2012). Incorporation of a horizontally transferred gene into an operon during cnidarian evolution. *PLoS One* 7, e31643.
- S3. Edelstein, A., Amodaj, N., Hoover, K., Vale, R., and Stuurman, N. (2010). Computer control of microscopes using μManager. *Curr. Protoc. Mol. Biol.* 92, 14.20.1-14.20.17.
- S4. Schindelin, J., Arganda-carreras, I., Frise, E., Kaynig, V., Longair, M., Pietzsch, T., Preibisch, S., Rueden, C., Saalfeld, S., Schmid, B., et al. (2012). Fiji : an open-source platform for biological-image analysis. *Nat. Methods* 9, 676–682.
- S5. Passano, L.M., and McCullough, C.B. (1964). Co-ordinating systems and behaviour in Hydra. I. Pacemaker system of the periodic contractions. *J. Exp. Biol.* 41, 643–664.
- S6. Passano, L.M., and McCullough, C.B. (1965). Co-ordinating systems and behaviour in Hydra. II. The rhythmic potential system.